AGU PUBLICATIONS

Geophysical Research Letters

RESEARCH LETTER

10.1002/2014GL059725

Key Points:
- Peculiar pitch angle distribution in the inner belt and slot region is reported
- Pitch angle distribution with minimum at 90° persists in inner belt
- Chorus/fast magnetosonic wave heating is suggested as a possible mechanism

Correspondence to:
H. Zhao,
hong.zhao@colorado.edu

Citation:
Zhao, H., X. Li, J. B. Blake, J. F. Fennell, S. G. Claudepierre, D. N. Baker, A. N. Jaynes, D. M. Malaspina, and S. G. Kanekal (2014), Peculiar pitch angle distribution of relativistic electrons in the inner radiation belt and slot region, *Geophys. Res. Lett.*, *41*, 2250–2257, doi:10.1002/2014GL059725.

Received 24 FEB 2014
Accepted 22 MAR 2014
Accepted article online 26 MAR 2014
Published online 7 APR 2014

Peculiar pitch angle distribution of relativistic electrons in the inner radiation belt and slot region

H. Zhao[1,2], X. Li[1,2], J. B. Blake[3], J. F. Fennell[3], S. G. Claudepierre[3], D. N. Baker[1], A. N. Jaynes[1], D. M. Malaspina[1], and S. G. Kanekal[4]

[1]Laboratory for Atmospheric and Space Physics, University of Colorado Boulder, Boulder, Colorado, USA, [2]Department of Aerospace Engineering Sciences, University of Colorado Boulder, Boulder, Colorado, USA, [3]The Aerospace Corporation, Los Angeles, California, USA, [4]Goddard Space Flight Center, Greenbelt, Maryland, USA

Abstract The relativistic electrons in the inner radiation belt have received little attention in the past due to sparse measurements and unforgiving contamination from the inner belt protons. The high-quality measurements of the Magnetic Electron Ion Spectrometer instrument onboard Van Allen Probes provide a great opportunity to investigate the dynamics of relativistic electrons in the low *L* region. In this letter, we report the newly unveiled pitch angle distribution (PAD) of the energetic electrons with minima at 90° near the magnetic equator in the inner belt and slot region. Such a PAD is persistently present throughout the inner belt and appears in the slot region during storms. One hypothesis for 90° minimum PADs is that off 90° electrons are preferentially heated by chorus waves just outside the plasmapause (which can be at very low *L* during storms) and/or fast magnetosonic waves which exist both inside and outside the plasmasphere.

1. Introduction

Relativistic electrons in the inner magnetosphere are distributed into two regions, the inner radiation belt and outer radiation belt, while the region separating the two belts is called the slot region ($2 < L < 3$). The inner radiation belt is thought to be quite stable and exhibits limited variations only during geomagnetic active time [e.g., *Baker and Blake*, 2013]. It has been reported that while MeV electron injections into the slot region are rare and mostly occur during strong storms and intense solar wind conditions [e.g., *Baker et al.*, 2007; *Li et al.*, 2009; *Zhao and Li*, 2013a], hundreds of keV electron injections and precipitation in the slot region and inner belt occur much more often [e.g., *Sauvaud et al.*, 2008; *Selesnick et al.*, 2013; *Zhao and Li*, 2013b].

However, the energetic electron pitch angle distribution (PAD) inside the slot region and inner radiation belt received little attention in the past. *Lyons et al.* [1972] studied whistler mode waves that caused pitch angle diffusion of energetic electrons within the plasmasphere and showed that the equatorial PAD for hundreds of keV electrons are expected to be like a normal distribution with a bump around 90°, which is similar to observations at $L = 3$–4 during the decay phase following an injection event. *Lyons and Williams* [1975a, 1975b] reported detailed PADs of 35–560 keV energetic electrons from Explorer 45 observations at $L = 2$–4. They found that during geomagnetic quiet time, the PADs in the slot region and outer regions of the plasmasphere near the magnetic equator observed by Explorer 45 can be primarily explained by resonance interactions with plasmaspheric hiss, while during active time, the PADs are greatly distorted because of injections, and during poststorm decay periods, 90° minima in the PADs at $L = 2$–4 were occasionally observed. Most other research efforts on the relativistic electron PADs focus on the outer belt region [e.g., *Gannon et al.*, 2007].

One reason for the lack of attention to the inner belt electrons during the past decades is the limited quality data available, mainly due to the contamination from the coexisting very energetic protons that can penetrate through most shielding. Now the newly available Radiation Belt Storm Probes (RBSP) - Energetic Particle, Composition, and Thermal Plasma (ECT) [*Spence et al.*, 2013] data from Magnetic Electron Ion Spectrometer (MagEIS) [*Blake et al.*, 2013] onboard the Van Allen Probes spacecraft [*Kessel et al.*, 2013] provide an unprecedented opportunity to study the detailed PADs for hundreds of keV electrons in the slot region and inner belt. In this letter, we focus on hundreds of keV electron measurements from MagEIS and report the newly unveiled electron PADs with minima at 90° in the inner radiation belt and slot region. Such kind of PADs, different from analytical results of wave-particle interaction [e.g., *Lyons et al.*, 1972], is present

©2014. American Geophysical Union. All Rights Reserved.

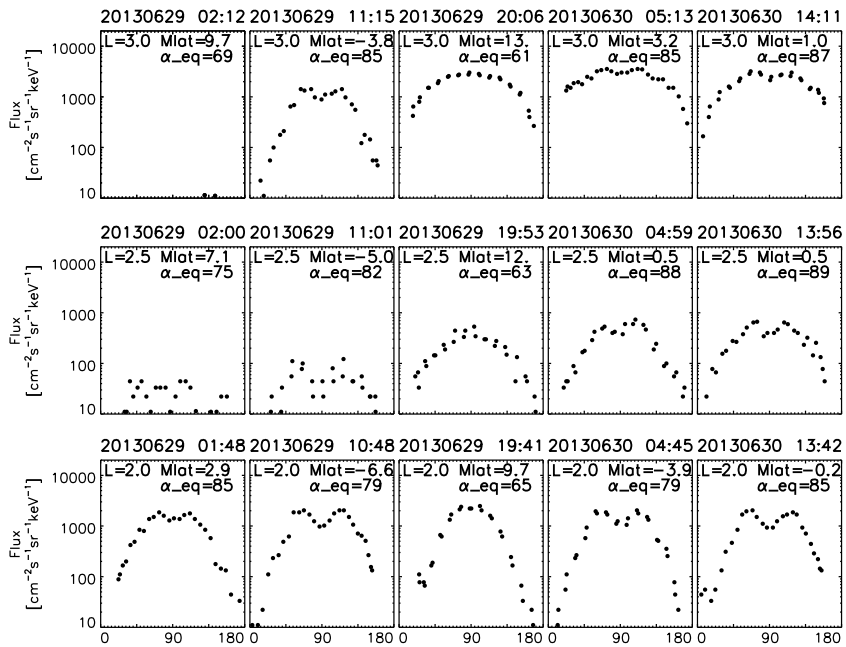

Figure 1. The pitch angle distributions of 464 keV electrons from Van Allen Probe-A during 29–30 June 2013, at (top) L = 3.0, (middle) 2.5, and (bottom) 2.0, respectively. Two parameters shown in the top right corner of each panel are magnetic latitude (MLAT) and the corresponding equatorial pitch angle of locally mirroring electrons (α_eq). The data are from outbound passes only.

throughout the inner belt and slot region and exhibits great variations during storm time in the slot region while remaining almost continuously present in the inner belt.

2. Observations

2.1. Storm Time

The PADs of 464 keV electrons at different L during 29–30 June 2013 are shown in Figure 1, in which all data are from the outbound passes only from Van Allen Probe-A in order to avoid any local time dependence. Three rows correspond to the PADs observed at L = 3.0, 2.5, and 2.0, respectively. Here we use McIlwain L with TS04 magnetic field model [*Tsyganenko and Sitnov*, 2005]. Two parameters are calculated and shown in the top right corner of each panel: magnetic latitude (MLAT) and the corresponding equatorial pitch angle of locally mirroring electrons (α_eq). This is a geomagnetic active time period, with a strong storm (minimum $Dst \sim -100$ nT and maximum $AE \sim 1200$ nT) occurring on June 28. There is a significant electron flux enhancement at $L = 2.5$ and above, while the flux level at $L = 2.0$ almost does not change. One significant signature here is that during this time period, the minima at 90° in PADs developed. At $L = 3.0$ and 2.5, we can see this 90° minima appeared along with the flux enhancement on June 29 and persist at least several orbits. At $L = 2.0$, the 90° minima was there earlier but became more significant as the flux enhancement occurred. It is worth mentioning that in the third column, no minimum at 90° is observed because the magnetic latitude is too high (almost no minimum at 90° is observed in the inner belt and slot region when $|\text{MLAT}| > \sim 10°$). The structure of minima at 90° is also present in lower energy channels (as low as 30 keV) but is less obvious. For the energy channels higher than 464 keV, the fluxes are too low and too close to the background to get clear PADs. *Lyons and Williams* [1975b] have reported this kind of structure that appeared around L =2–4 during some poststorm time periods. However, they described this kind of structures as short lived (8–24 h) and only present during active period. The short-lived feature they described probably is because they did not take into consideration the magnetic latitude. As shown in Figure 1, when the corresponding equatorial pitch angle of locally mirroring particles is high enough, we can always see this kind of PAD. Though not shown here, PADs with minima at 90° can last for days at the outer edge of the slot region and for over a year in the heart of inner radiation belt according to Van Allen Probes observations. Another aspect in contrast to what *Lyons and Williams* [1975b] mentioned is that minima at 90° in PADs do exist during the quiet time as well, as shown in Figure 2.

©2014. American Geophysical Union. All Rights Reserved.

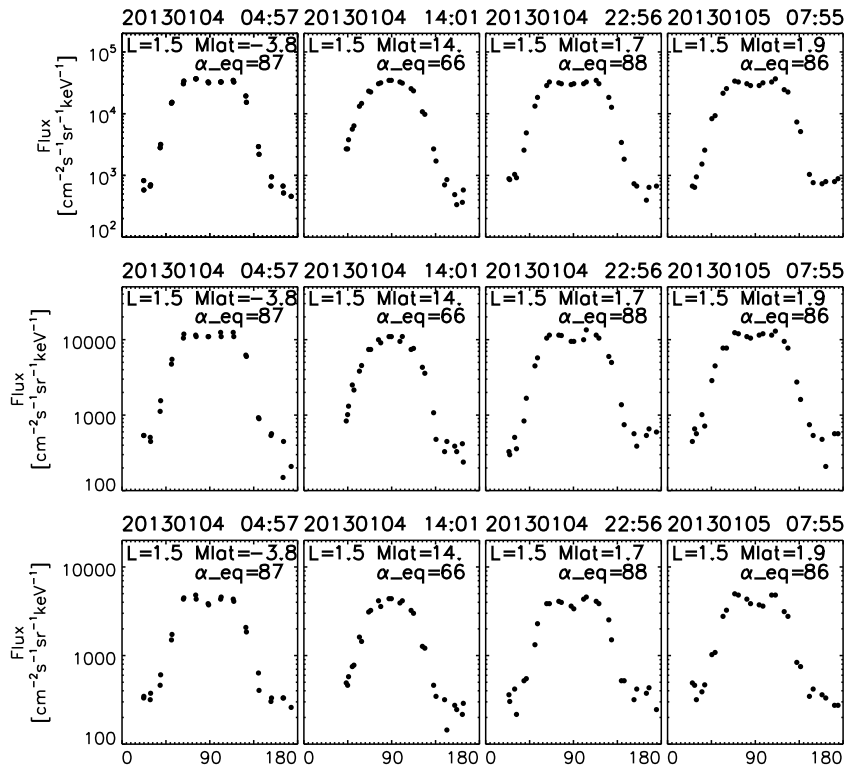

Figure 2. The PADs of (top) 237 keV, (middle) 349 keV, and (bottom) 456 keV electrons, respectively, at $L = 1.5$ during 4–5 January 2013. The data are from inbound passes of Van Allen Probe-A only.

2.2. Quiet Time

Figure 2 shows the PADs at $L = 1.5$ during 4–5 January 2013, a geomagnetic quiet time period ($Dst \sim 0$ nT and $AE < 200$ nT), for three different energy channels (237 keV, 349 keV, and 456 keV from the top to bottom, respectively). The format of Figure 2 is similar to that of Figure 1, but only the inbound passes from Van Allen Probe-A are plotted. It is clear that during this quiet time period, with passes close enough to the magnetic equator, PADs with minima at 90° are always observed, and the situation is similar for all three energy channels. Figure 2 suggests that PADs with 90° minima are generally present in the inner radiation belt, even during very quiet time period. In the slot region, however, this kind of PADs is not clearly observed at $L = 2.0$–2.5 during this time period; at larger L the fluxes are low and close to background levels, and thus, no clear PAD patterns are measured.

2.3. Statistics

In order to show the general features of PADs with minima at 90° over time and L, we developed a program to automatically identify this kind of PAD inside the inner belt and slot region and then calculated the frequency of occurrence. The criteria we used include (1) $f_{avg}(85° : 95°) < 0.95 \times f_{avg}(90° - \alpha : 90° + \alpha)$, where $f_{avg}(a : b)$ is the averaged flux of electrons with pitch angle between a and b and α is selected from 5° to 45° to maximize the value of $f_{avg}(90° - \alpha : 90° + \alpha)$ and (2) total square root of counts (summed over all pitch angles) is greater than 50. We only included those points when the satellite is close enough to the magnetic equator (the corresponding equatorial pitch angle of locally mirroring electrons is greater than 85°) in the statistics. Using these criteria, we plotted the frequency of occurrence of PADs with 90° minima of ~460 keV electrons over a year as a function of L and time in Figure 3 using data from both probes. Figure 3 also includes the daily averaged *Dst* and *AE* indices measured (real time) in black and predicted in red [*Temerin and Li*, 2002, 2006; *Li et al.*, 2007, *Luo et al.*, 2013]. The color bar in Figure 3 (top) indicates the frequency of occurrence of PADs with minima at 90°, where red means this kind of PADs is always observed and black means no such kind of PADs. The white regions are where the second criterion cannot be met, or both satellites are away from the magnetic equator. It is clear that for ~460 keV electrons, at $L = 1.5$, this kind of PAD is always observed and has almost no correlation with geomagnetic activity; but at $L = \sim 1.8$–3.0, the occurrence of PADs with 90° minima is strongly correlated with both the AE and *Dst* indices. During the

©2014. American Geophysical Union. All Rights Reserved.

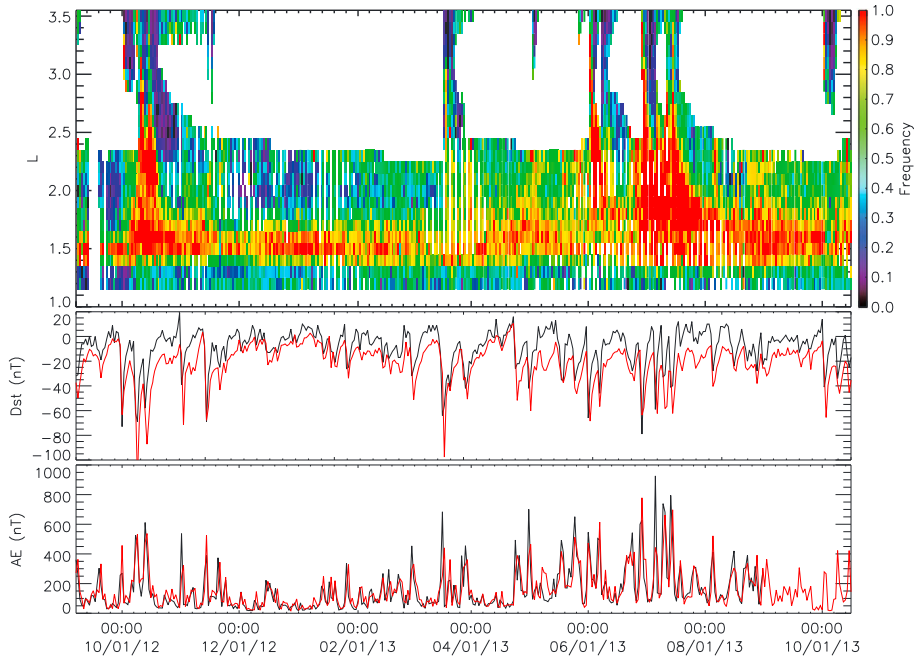

Figure 3. (top) The frequency of occurrence of PADs with minima at 90° of ~460 keV electrons as a function of *L* and time from September 2012 to October 2013. (middle) The daily averaged real-time *Dst* index (black) and predicted *Dst* index (red). (bottom) The daily averaged real-time *AE* index (black) and predicted *AE* index (red).

quiet time, e.g., December 2012 to February 2013, PADs with minima at 90° are rarely observed at and above $L = 1.8$, while during the active time, e.g., in July 2013, the frequency of occurrence of PADs with minima at 90° between $L = 1.8$–2.5 is very high. Also, after such PAD pattern is initially created, it lasts longer at lower *L*, and disappears faster at higher *L*.

2.4. Averaged PAD

It is also important to show the averaged PADs during quiet and active time and at different *L*, respectively. As an example, we calculate the averaged PADs of ~460 keV electrons during a geomagnetic quiet month (December 2012, Figure 4 (top)) and active month (July 2013, Figure 4 (bottom)), respectively, at $L = 1.5$, 1.8, 2.0, and 2.3 (with $\Delta L = 0.05$) for comparison. The number of PADs being averaged is shown in the top right corner of each panel. Similarly, here we also use the PADs measured by both probes but only when the

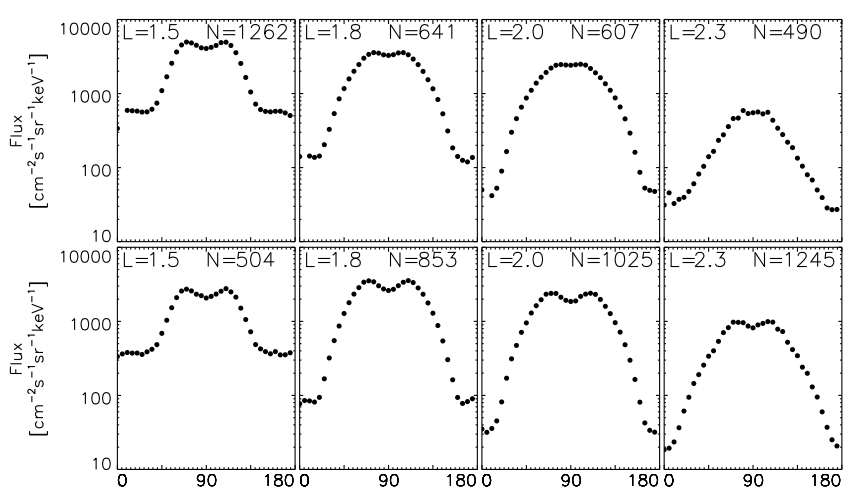

Figure 4. The averaged PADs of ~460 keV electrons during geomagnetic (top) quiet (December 2012) and (bottom) active times (July 2013), respectively, at $L = 1.5$, 1.8, 2.0, and 2.3, using data from both probes. The *L* is shown in the top left corner for each panel, while the number of PADs being averaged is shown in the top right corner.

©2014. American Geophysical Union. All Rights Reserved.

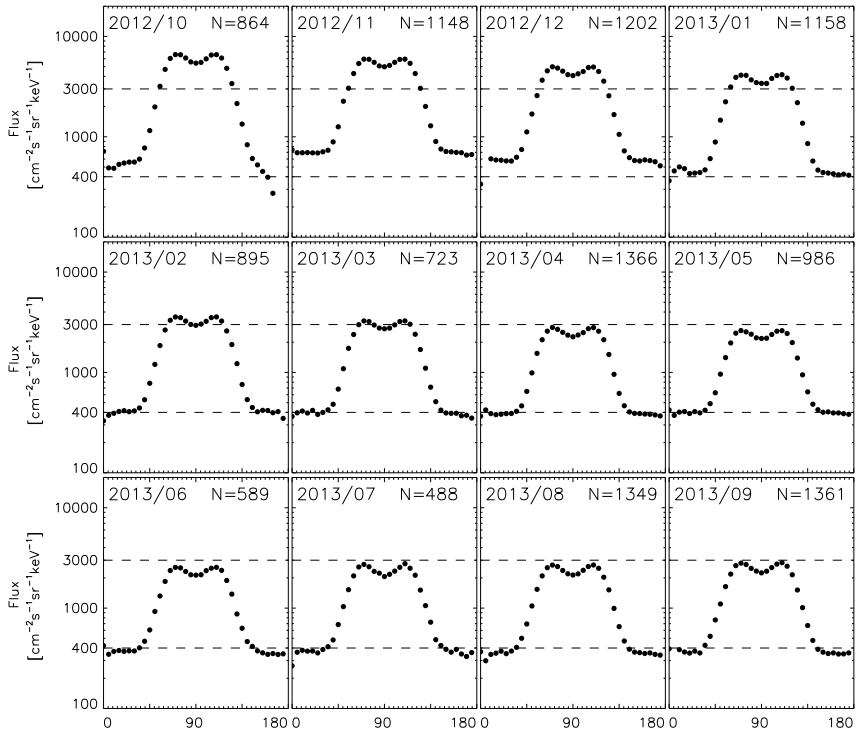

Figure 5. The monthly averaged PADs of ~460 keV electrons at L = 1.5, from October 2012 to September 2013, using data from both probes. The number of PADs being averaged is shown in the top right corner of each panel. The two dashed lines in each panel are just for reference.

probe is close enough to the magnetic equator with α_eq > 85°. The results are clear and significant: during active time, the PADs with minima at 90° are present throughout the slot region and inner belt; during quiet time, such kind of PADs is still present in the inner belt but much less obvious in the slot region. Also, by comparing the averaged PADs at different L, we see that, at $L = 1.5$, the structure almost does not change, while at $L > 1.8$, the structure is less significant during quiet time and more notable during active time. As L increases, the minimum at 90° disappears during quiet time. One thing notable is that we can clearly see from Figure 4 that the flux level inside the loss cone is high at $L = 1.5$ and gradually decreases as L increases, which is likely due to the contamination of the inner belt protons. However, since the peak flux values are at least 1 order of magnitude higher than the background fluxes, such background should not affect the PADs near 90° for ~460 keV electrons.

It should be interesting to look at the long-term behavior of PADs in the inner belt. Figure 5 shows the monthly averaged PADs of ~460 keV electrons at $L = 1.5$, from October 2012 to September 2013 using the same criterion as in Figure 4. The situation is similar but confirming: the 90° minima in the averaged PADs persist all the time, and the shapes of PADs did not change much over the whole year at $L = 1.5$. It is also worth mentioning that during the first 6 months of the mission, there are several gain changes and energy channels changes, which makes the backgrounds and the peak values of the measurements in the PADs change but not the PAD shape itself. During the next 6 months, it is clear that the flux level and PADs at $L = 1.5$ almost did not change, even during active time. This suggests that in the heart of inner belt, the flux of hundreds of keV electrons does not change much as expected from the low scattering rates by plasmaspheric hiss waves at low L region [e.g., *Abel and Thorne*, 1998] (unless there are much stronger magnetic storms, e.g., 24–25 March 1991 and 30–31 October 2003), and PADs with minima at 90° are always expected.

To summarize, we found that the PADs inside the inner radiation belt and slot region are different from predictions of previous theories [e.g., *Lyons et al.*, 1972]; actually, near the magnetic equator, the pitch angle distributions with minima at 90° are always observed in the inner belt and are expected in the slot region during storm times. The PADs with minima at 90° have several features: (1) during the geomagnetic active times, such kind of PADs is almost always present inside the inner belt and slot region; (2) during the geomagnetic quiet times, such kind of PADs also exists in the inner belt but is much less significant in the slot

©2014. American Geophysical Union. All Rights Reserved.

region; and (3) the minima at 90° in PADs can last for several days to months in the inner belt and slot region, depending on L, and this structure disappears faster with increasing L, possibly due to stronger pitch angle scattering by whistler mode hiss waves at higher L [e.g., *Abel and Thorne*, 1998; *Artemyev et al.*, 2013].

We did not find any significant longitude dependence or local time dependence at this time (though this may be because we do not have enough data coverage yet).

3. Discussion

The electron PAD is determined by both the source and loss processes. The most important source processes for the inner belt particles were recognized to be cosmic ray albedo neutron decay (CRAND) and inward radial diffusion. Radial diffusion energizes electrons by bringing them inward while conserving the first and second adiabatic invariants [e.g., *Schulz and Lanzerotti*, 1974], which causes the enhancement of perpendicular energy and likely leads to a 90° peaked PAD. As for CRAND, many studies suggest that it is an important source for energetic protons in the inner belt but not for the electrons [e.g., *Kellogg*, 1960; *Pizzella et al.*, 1962]. The loss processes for the inner belt and slot region electrons include Coulomb collisions with atmospheric constituents and pitch angle scattering. Atmospheric collisions dominate energetic electron loss only for $L < 1.3$ [*Walt*, 1964; *Selesnick*, 2012]; above $L = 1.3$ wave-particle interaction, caused by plasmaspheric hiss, lightning-induced whistlers, and whistlers due to VLF transmitters, plays an important role in the loss of energetic electrons [e.g., *Abel and Thorne*, 1998; *Blake et al.*, 2001]. Because of the nature that in the inner belt and slot region wave-particle interaction is not efficient for near equatorially mirroring electrons, one would expect a highly 90° peaked PAD inside the inner belt and slot region [e.g., *Lyons et al.*, 1972; *Lyons and Williams*, 1975a, 1975b].

However, the newly unveiled observations from MagEIS onboard Van Allen Probes show the opposite. One possible explanation for the PADs with 90° minima is that the chorus wave heating, right outside the plasmapause, is more efficient for off-equator electrons [e.g., *Horne et al.*, 2005]. During active time, the plasmasphere shrinks and the plasmapause can reach very low L, sometimes as low as $L = 2$ [e.g., *Baker et al.*, 2004] or even lower [e.g., *O'Brien and Moldwin*, 2003]. Right outside the plasmapause, off-equator electrons are preferentially accelerated by chorus waves and the 90° minimum PAD is created. After the storm, the plasmasphere expands and whistler mode waves take effect inside plasmasphere, scattering electrons into the loss cone. However, whistler mode waves are not efficient scattering hundreds of keV electrons with $\alpha_{eq} \sim 60°–80°$ in the low L region [e.g., *Abel and Thorne*, 1998; *Shprits*, 2009]. Thus, the PAD pattern persists in the inner belt and gradually disappears in the slot region. It is worth pointing out that the plasmapause location can be much more dynamic and reach much lower L during storms than one would think. For example, during 29 June 2013 (minimum *Dst* is about −100 nT), a plasmapause crossing was seen at $L \sim 2.56$. In this case, the plasmapause crossing was evident in the Electric Field and Wave instrument data [*Wygant et al.*, 2013] as a sharp change in the spacecraft potential of Van Allen Probe-A simultaneously observed with abrupt onset of plasmaspheric hiss. Because each Van Allen Probes' orbit only crosses the plasmapause twice every 9 h (nominally, assuming a plasmasphere eroded to $L < 6$), plasmapause dynamics are undersampled in time, and the lowest plasmapause location may have been even closer to Earth than $L \sim 2.56$ for this event. This hypothesis is consistent with the fact that such kind of PADs occurs during strong storms and gradually disappears after several days or months, with higher disappearance rate at larger L. Besides chorus waves, fast magnetosonic waves could also be a potential mechanism causing 90° minimum PAD in the low L region. Fast magnetosonic waves, which exist both outside and inside the plasmasphere and are much stronger under disturbed conditions [e.g., *Ma et al.*, 2013], have been shown as an effective local acceleration mechanism and can accelerate tens of keV to a few MeV electrons with the energy diffusion rates maximizing between $\alpha_{eq} = 60°–80°$ [e.g., *Horne et al.*, 2007; *Mourenas et al.*, 2013]. Thus, they could possibly create 90° minimum PAD by preferentially heating off-equator electrons too. Another hypothesis is that inward radial diffusion can bring some electrons to lower L while preserving the PAD pattern created by chorus/fast magnetosonic wave heating, since in the inner belt and slot region, the positive radial gradient of the phase space density in the inner belt and slot region for given first and second adiabatic invariants is often observed during storms. To fully understand the cause of PADs with minima at 90° in the low L region, some detailed modeling is needed, but this is beyond the scope of this letter.

©2014. American Geophysical Union. All Rights Reserved.

4. Conclusion

A detailed analysis of the PADs of relativistic electrons in the inner belt and slot region has been performed based on the newly available MagEIS measurements. A peculiar pattern of 90° minimum PAD, which is very different from previous theoretical predictions, has been identified. This pattern of PADs is a persistent feature in the inner belt and appears in the slot region during geomagnetic active time. A hypothesis is proposed to interpret the observations: off 90° electrons are preferentially heated by chorus waves right outside the plasmapause (which can be at very low L during storm times) and/or fast magnetosonic waves which exist both inside and outside the plasmasphere. After being created, the pattern of PADs is preserved as the plasmasphere expands and gradually disappears in the slot region due to pitch angle scattering by whistler mode waves. Detailed modeling is required to fully understand the physical cause. Regardless, the newly unveiled feature, made possible by the high-quality measurements of MagEIS, is compelling.

Acknowledgments
We would like to thank Richard Selesnick and Mike Temerin, Lauren Blum, Quintin Schiller, and Sam Califf for helpful discussions. This work is mainly supported by NSF (CubeSat program) grant AGSW 0940277, NASA grant NNX10AQ48G, and NASA contract NAS5-01072 (Van Allen Probes mission). We thank the World Data Center for Geomagnetism, Kyoto, for providing *Dst* and *AE* indices. The predicted *Dst* and *AE* indices are available at http://lasp.colorado.edu/space_weather/dsttemerin/dsttemerin.html.

The Editor thanks Jay Albert and an anonymous reviewer for their assistance in evaluating this paper.

References

Abel, B., and R. M. Thorne (1998), Electron scattering loss in Earth's inner magnetosphere 1. Dominant physical processes, *J. Geophys. Res.*, *103*(A2), 2385–2396.

Artemyev, A., D. Mourenas, O. Agapitov, and V. Krasnoselskikh (2013), Parametric validations of analytical lifetime estimates for radiation belt electron diffusion by whistler waves, *Ann. Geophys.*, *31*, 599–624.

Baker, D. N., S. G. Kanekal, X. Li, S. P. Monk, J. Goldstein, and J. L. Burch (2004), An extreme distortion of the Van Allen belt arising from the 'Hallowe'en' solar storm in 2003, *Nature*, *432*, 878–881.

Baker, D. N., S. G. Kanekal, R. B. Home, N. P. Meredith, and S. A. Glauert (2007), Low-altitude measurements of 2-6 MeV electron trapping lifetimes at $1.5 < L < 2.5$, *Geophys. Res. Lett.*, *34*, L20110, doi:10.1029/2007GL031007.

Baker, D. N., and J. B. Blake (2013), SAMPEX: A long-serving radiation belt sentinel, in *Dynamics of the Earth's Radiation Belts and Inner Magnetosphere*, edited by D. Summers et al., AGU, Washington, D. C., doi:10.1029/2012GM001368.

Blake, J. B., U. S. Inan, M. Walt, T. F. Bell, J. Bortnik, D. L. Chenette, and H. J. Christian (2001), Lightning-induced energetic electron flux enhancements in the drift loss cone, *J. Geophys. Res.*, *106*(A12), 29,733–29,744.

Blake, J. B., et al. (2013), The magnetic electron ion spectrometer (MagEIS) instruments aboard the radiation belt storm probes (RBSP) spacecraft, *Space Sci. Rev.*, *179*(1-4), 383–421, doi:10.1007/s11214-013-9991-8.

Gannon, J. L., X. Li, and D. Heynderickx (2007), Pitch angle distribution analysis of radiation belt electrons based on Combined Release and Radiation Effects Satellite Medium Electrons A data, *J. Geophys. Res.*, *112*, A05212, doi:10.1029/2005JA011565.

Horne, R. B., R. M. Thorne, S. A. Glauert, J. M. Albert, N. P. Meredith, and R. R. Anderson (2005), Timescale for radiation belt electron acceleration by whistler mode chorus waves, *J. Geophys. Res.*, *110*, A03225, doi:10.1029/2004JA010811.

Horne, R. B., R. M. Thorne, S. A. Glauert, N. P. Meredith, D. Pokhotelov, and O. Santolik (2007), Electron acceleration in the Van Allen radiation belts by fast magnetosonic waves, *Geophys. Res. Lett.*, *34*, L17107, doi:10.1029/2007GL030267.

Kellogg, P. J. (1960), Electrons of the Van Allen radiation, *J. Geophys. Res.*, *65*(9), 2705–2713.

Kessel, R. L., N. J. Fox, and M. Weiss (2013), The Radiation Belt Storm Probes (RBSP) and space weather, *Space Sci. Rev.*, *179*(1-4), 531–543, doi:10.1007/s11214-012-9953-6.

Li, X., K. S. Oh, and M. Temerin (2007), Prediction of the AL index using solar wind parameters, *J. Geophys. Res.*, *112*, A06224, doi:10.1029/2006JA011918.

Li, X., A. B. Barker, D. N. Baker, W. Tu, T. E. Sarris, R. S. Selesnick, R. Friedel, and C. Shen (2009), Modeling the deep penetration of outer belt electrons during the "Halloween" magnetic storm in 2003, *Space Weather*, *7*, S02004, doi:10.1029/2008SW000418.

Luo, B., X. Li, M. Temerin, and S. Liu (2013), Prediction of the AU, AL, and AE indices using solar wind parameters, *J. Geophys. Res. Space Physics*, *118*, 7683–7694, doi:10.1002/2013JA019188.

Lyons, L. R., R. M. Thorne, and C. F. Kennel (1972), Pitch-angle diffusion of radiation belt electrons within the plasmasphere, *J. Geophys. Res.*, *77*(19), 3455–3474.

Lyons, L. R., and D. J. Williams (1975a), The quiet time structure of energetic (35-560 keV) radiation belt electrons, *J. Geophys. Res.*, *80*(7), 943–950.

Lyons, L. R., and D. J. Williams (1975b), The storm and poststorm evolution of energetic (35-560 keV) radiation belt electron distributions, *J. Geophys. Res.*, *80*(28), 3985–3994.

Ma, Q., W. Li, R. M. Thorne, and V. Angelopoulos (2013), Global distribution of equatorial magnetosonic waves observed by THEMIS, *Geophys. Res. Lett.*, *40*, 1895–1901, doi:10.1002/grl.50434.

Mourenas, D., A. V. Artemyev, O. V. Agapitov, and V. Krasnoselskikh (2013), Analytical estimates of electron quasilinear diffusion by fast magnetosonic waves, *J. Geophys. Res. Space Physics*, *118*, 3096–3112, doi:10.1002/jgra.50349.

O'Brien, T. P., and M. B. Moldwin (2003), Empirical plasmapause models from magnetic indices, *Geophys. Res. Lett.*, *30*(4), 1152, doi:10.1029/2002GL016007.

Pizzella, G., C. D. Laughlin, and B. J. O'Brien (1962), Note on the electron energy spectrum in the inner Van Allen belt, *J. Geophys. Res.*, *67*(9), 3281–3287.

Sauvaud, J. A., R. Maggiolo, C. Jacquey, M. Parrot, J. J. Berthelier, R. J. Gamble, and C. J. Rodger (2008), Radiation belt electron precipitation due to VLF transmitters: Satellite observations, *Geophys. Res. Lett.*, *35*, L09101, doi:10.1029/2008GL033194.

Schulz, M., and L. Lanzerotti (1974), *Particle Diffusion in the Radiation Belts*, Springer, New York.

Selesnick, R. S. (2012), Atmospheric scattering and decay of inner radiation belt electrons, *J. Geophys. Res.*, *117*, A08218, doi:10.1029/2012JA017793.

Selesnick, R. S., J. M. Albert, and M. J. Starks (2013), Influence of a ground-based VLF radio transmitter on the inner electron radiation belt, *J. Geophys. Res. Space Physics*, *118*, 628–635, doi:10.1002/jgra.50095.

Shprits, Y. Y. (2009), Potential waves for pitch-angle scattering of near-equatorially mirroring energetic electrons due to the violation of the second adiabatic invariant, *Geophys. Res. Lett.*, *36*, L12106, doi:10.1029/2009GL038322.

Spence, H. E., et al. (2013), Science goals and overview of the energetic particle, composition, and thermal plasma (ECT) suite on NASA's radiation belt storm probes (RBSP) mission, *Space Sci. Rev.*, *179*(1-4), 311–336, doi:10.1007/s11214-013-0007-5.

©2014. American Geophysical Union. All Rights Reserved.

Temerin, M., and X. Li (2002), A new model for the prediction of Dst on the basis of the solar wind, *J. Geophys. Res.*, *107*(A12), 1472, doi:10.1029/2001JA007532.

Temerin, M., and X. Li (2006), Dst model for 1995-2002, *J. Geophys. Res.*, *111*, A04221, doi:10.1029/2005JA011257.

Tsyganenko, N. A., and M. I. Sitnov (2005), Modeling the dynamics of the inner magnetosphere during strong geomagnetic storms, *J. Geophys. Res.*, *110*, A03208, doi:10.1029/2004JA010798.

Walt, M. (1964), The effects of atmospheric collisions on geomagnetically trapped electrons, *J. Geophys. Res.*, *69*(19), 3947–3958.

Wygant, J. R., et al. (2013), The Electric Field and Waves (EFW) Instruments on the Radiation Belt Storm Probes Mission, *Space Sci. Rev.*, *179*, 183–220, doi:10.1007/s11214-013-0013-7.

Zhao, H., and X. Li (2013a), Inward shift of outer radiation belt electrons as a function of Dst index and the influence of the solar wind on electron injections into the slot region, *J. Geophys. Res. Space Physics*, *118*, 756–764, doi:10.1029/2012JA018179.

Zhao, H., and X. Li (2013b), Modeling energetic electron penetration into the slot region and inner radiation belt, *J. Geophys. Res. Space Physics*, *118*, 6936–6945, doi:10.1002/2013JA019240.

©2014. American Geophysical Union. All Rights Reserved.